DOI: 10.6060/mhc245844k

Spectral-Luminescent and Photophysical Properties of Free Base Corroles

Mikalai M. Kruk,[a@] Dmitry V. Klenitsky,[a] and Lev L. Gladkov[b]

[a]*Belarusian State Technological University, Physics Department, 220006 Minsk, Belarus*
[b]*Belarusian State Academy of Communications, Department of Physical and Mathematical Basis of Informatics, 220114 Minsk, Belarus*
[@]*Corresponding author E-mail: krukmikalai@yahoo.com; m.kruk@belstu.by*

Dedicated to the 80th anniversary of Academician O. I. Koifman and to the 95th anniversary of Founder of the Ivanovo macroheterocyclic chemistry school B. D. Berezin

Corroles are the brightest representatives of the contracted tetrapyrrolic macrocycles whose electronic structure, spectral-luminescent and photophysical properties are quite different from those of porphyrins. To date the number of reviews has appeared dealing with the synthesis and applications studies, but much less attention has been paid to the results of the fundamental studies on the electronic structure, aromaticity and photophysics of these compounds. This review aims to summarize the peculiarities of the spectral-luminescent and photophysical properties of the free base corroles unraveled in last twenty years.

Keywords: Free base corroles, π–conjugation, absorption, fluorescence, phosphorescence, excited state deactivation.

Спектрально-люминесцентные и фотофизические свойства свободных оснований корролов

Н. Н. Крук,[a@] Д. В. Кленицкий,[a] Л. Л. Гладков[b]

[a]*УО «Белорусский государственный технологический университет», 220006 Минск, Беларусь*
[b]*УО «Белорусская государственная академия связи», 220114 Минск, Беларусь*
[@] *E-mail: krukmikalai@yahoo.com; m.kruk@belstu.by*

Посвящается 80-летию со дня рождения Академика О. И. Койфмана и 95-летию со дня рождения основателя Ивановской школы химии макрогетероциклических соединений Б. Д. Березина

Корролы — ярчайшие представители сокращенных тетрапиррольных макроциклов, электронная структура, спектрально-люминесцентные и фотофизические свойства которых существенно отличаются от порфиринов. К настоящему времени появился ряд обзоров, посвященных синтезу и прикладным исследованиям, однако результатам фундаментальных исследований электронного строения, ароматичности и фотофизики этих соединений уделяется гораздо меньшее внимание. Целью данного обзора является обобщение выявленных за последние двадцать лет особенностей спектрально-люминесцентных и фотофизических свойств свободных оснований корролов.

Ключевые слова: Свободные основания корролов, π–сопряжение, поглощение, флуоресценция, фосфоресценция, дезактивация возбужденных состояний.

Electronic Structure, Aromaticity and π–Conjugation

Corroles constitute the family of contracted tetrapyrrolic compounds due to lacking of one methine bridge in the macrocycle, and the C_a-C_a bond connects the pair of adjacent pyrrole rings. Lacking one methine bridge would decrease the number of π-electrons in the corrole macrocycle, but the imine to amine rearrangement takes place for the nitrogen atom in one of the pyrrole rings. Having the same sp^2 hybridization as C_m-carbon has, the amine nitrogen has two p_z-electrons to donate into conjugated π-system in contrast with only one for the imine nitrogen. Because of such rearrangement, the total number of π-electrons in the corrole macrocycle remains the same as in the porphyrin macrocycle, namely 26 π-electrons. Therefore, the free base corroles are isoelectronic with the free base porphyrins and also fulfill the Hückel rule for the macrocycle aromaticity, requiring the macrocycle to have the $(4n + 2)$ π-electrons, where n is an integer. However, the corrole macrocycle possesses the higher electron density compared to that of the porphyrin since the same number of π-electrons distribute over lower number of skeletal macrocyclic atoms.[1] At the same time, it was proposed that π-electron density has non-uniform distribution over the macrocycle due to decrease in the molecular symmetry of the free base corrole molecule down to C_{2v} (C_s) compared to the D_{2h} for the free base porphyrin.[2] The dipyrrole unit of the macrocycle is suggested to be more electron rich, whereas dipyrromethene unit has lower electron density. These differences are expected to affect the macrocycle aromaticity.[1]

The evaluation of the aromaticity of the contracted corrole macrocycle is nontrivial problem. The imine to amine rearrangement in the corrole macrocycle causes the intrinsic macrocycle nonplanarity due to pronounced steric hindrances of three protons in the macrocyclic core. The type of the nonplanar distortions and its degree depend on the architecture of the peripheral substitution. This issue has been discussed in detail recently.[3] Another consequence of the rearrangements in the macrocycle core is the ultimate coexistence of NH-tautomers, which may undergo mutual transformations in the ground and excited electronic states. Although NH-tautomers are isoelectronic, the electron density distribution over the macrocycle being different, and provides the basis for the formation of different π-conjugation pathways, which, in their own turn, affect the aromaticity.

The aromaticity of the macroheterocyclic systems has hierarchical character. Aromatic pyrrole rings possessing the (local) aromaticity themselves are involved into formation of π-electron system of the macrocycle, whose aromaticity is the key element of the electronic structure of molecule. The planar configuration of all the subunits of the macroheterocyclic molecule favors the π-electron conjugation, but the free base corrole macrocycle is intrinsically nonplanar.[3] The saddling dihedrals χ_i between the pairs of adjacent pyrrole rings may amount of up to 88.7°,[4] providing extremely poor conditions for the π–orbitals overlap. On the level of local aromaticity of the pyrrole rings the deviations from planarity have been reported repeatedly (in fact, it was a reason of introducing two sets of (outer χ_i and inner χ'_i) saddling dihedrals). Then, the nitrogen pyramidalization was found to take place for all the pyrrole rings,[3,5-6] which also disfavors π-orbitals overlap within pyrrole rings. The nonplanar distortions of macrocycle are able to modulate the conjugation via changes of the valence angles between skeletal atoms along the macrocycle.

There are several variants of the π-conjugation pathways in the corrole macrocycle with 8 bifurcation points. According to the Hückel rule, one can suggest the pathways family containing 26, 22 or 18 π-electrons. Taking into account the macrocycle asymmetry, the architecture of the peripheral substitution and NH-tautomerization, the total number of possible conjugation pathways differs. Thus, in case of C_m-substitution with symmetrical A_3 and A_2B patterns, or C_b-substitution with symmetrical substitution of *AB* and *CD* pairs of pyrrole rings, the total number of different π-conjugation pathways will be 8. According to the concept proposed recently, all the macrocycle atoms participate in the formation of conjugated π-system, but with different weights,[7] the conjugation pathway to be the linear combination of these above-mentioned 8 pathways.

The molecular conformation optimization with density functional theory (DFT) methods and the harmonic oscillator model of aromaticity (HOMA) have been combined to identify the most probable π-conjugation pathway in the corrole macrocycle and to evaluate the aromaticity degree.[8,9] Substantially different participation of the macrocycle skeletal atoms in formation of the π-conjugation pathway has been established, and it was proposed that pathways consisting of 18 π-electrons were dominating for both NH-tautomers. It was found that the degree of aromaticity depends on both NH-tautomer structure and the architecture of the peripheral substitution for each of two tautomers, which possess its own dominating π-conjugation pathway, which consists of the dipyrromethene fragment. In the ground S_0 state the aromaticity of the long wavelength T1 tautomer (aromaticity index I_{HOMA}= 0.600 – 0.665) is slightly higher compared the that of the short wavelength T2 tautomer (I_{HOMA} = 0.590 – 0.642) for different architecture of peripheral substitution.[9]

Authors have suggested and experimentally proved the method of the control over the equilibrium between two NH-tautomers, which consisted in design of the specific electronic density distribution reflecting the π-conjugation pathway of given NH-tautomer by means of the peripheral substitution macrocycle. Provided that π-conjugation pathways differ for two NH-tautomers, such tautomers should form preferably and the NH-tautomeric equilibrium shifts in the direction of its stabilization. The increase in the degree of aromaticity also contributes to the stabilization of given NH-tautomer. The dominating π-conjugation pathways for two NH-tautomers are shown in Figure 1. One should notice, that the dominating π-conjugation pathway of the T2 tautomer does not depend on the substitution architecture among the studied compounds, whereas two (or even three) π-conjugation pathways reveal very close aromaticity index I_{HOMA} for the T1 tautomer as a function of the substitution pattern.

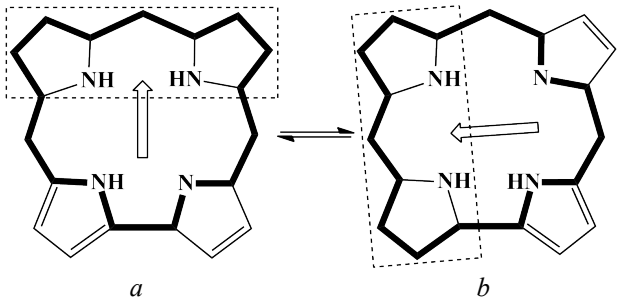

Figure 1. NH-tautomer equilibrium of the free base corroles: a) long wavelength T1 tautomer; b) short wavelength T2 tautomer. Dominating 18-membered conjugation pathways for the tautomers are shown with solid line.[8] Dotted rectangles represent the dipyrromethene fragments of the macrocycle involved into the conjugation. The arrows indicate the direction of the electron density shift in the macrocycle.

The Baird rule[10] on the inversion of the aromaticity in the excited (either S_1 or T_1) state have been proven to hold in case of the free base corroles.[9] The dominating π-conjugation pathways differ for NH-tautomers, but in the ground singlet S_0 and excited triplet T_1 states the dominating π-conjugation pathways for each of the tautomers keep the same. The estimated with I_{HOMA} index aromaticity degree in the triplet T_1 state decreased distinctly compared to the ground S_0 state. The aromaticity index I_{HOMA}= 0.475 – 0.547 in the lowest triplet T_1 state was found to be of the same order of magnitude as that for the norcorrole derivatives in the ground S_0 state and hexaphyrin derivatives in the lowest triplet T_1 state, which are known to be antiaromatic. Therefore, the conclusion has been made that the free base corrole tautomers undergo the aromaticity inversion upon excitation into the lowest triplet T_1 state.[9]

The Formation of the Ground State Absorption Spectra

The free base corrole electronic structure differs substantially from that of the porphyrins, however, in spite of these differences listed above, the basic principles underlying the aromaticity and electronic structure of the free base corroles seem to be the same in both cases. Starting from the very first spectroscopic studies the similar pattern of the ground state absorption spectra of the corroles and porphyrins has been noticed. The spectra were shown to have the weak absorption bands in the visible range and the strong (or stronger) Soret band at the edge of visible and ultraviolet spectral ranges.[11-12] These circumstances have damped the interest to the deep studies of the electronic structure and interpretation of the electronic absorption spectra for about 40 years after the discovery of corrole molecules.[6,13-15] Instead to elucidate the peculiarities of the spectral-luminescent properties of the free base corrole, most of the authors limited themselves to mentioning that "the spectral properties of the studied free base corroles being similar to those of the free base porphyrins".

A distinguishing feature of free base corroles is the distinct dependence of absorption band maxima in the electronic absorption spectra as well as their relative intensities on the nature of the solvent.[5-6,11,16-19 and Refs. therein] The spectra are often characterized by strongly overlapping bands that form broad structureless contours. This spectral pattern is contrasting with the absorption spectra of the free base porphyrins, which have well-resolved bands of both electronic and vibronic transitions in the visible and near-UV regions and very weak spectral shifts upon changing the solvent.[20] Several reasons leading to the above features of free-base corrole absorption spectra have now been established.

First of all, the contracted macrocycle of free base corroles is asymmetric because one C*m* carbon atom is missing. Thus, the macrocycle core contains three protons. This causes the free base corroles ultimately form the NH tautomers and, correspondingly, absorption spectra of their solutions to appear as superimposed absorption spectra of the NH tautomers.[5,6,14,16-18] The key point for the interpretation the ground state absorption spectrum consisted in the proposal to consider the spectrum of the free base corrole solution as two superimposed spectra belonging to pair of the NH-tautomers. The detailed interpretation of the ground state absorption spectra of the free base corroles in solutions has been obtained for the first time in the series of papers of Kruk and Maes *et al.*,[5-6,16-17,21] where combining of the four-orbital model of Gouterman and DFT quantum-chemical calculations has been used. Although the four-orbital model initially has been developed strictly for the porphyrins,[20-21] it was shown later that it holds too in case of the corrole macrocycles.[22-23] The four-orbital model expects that there are four electronic transitions for a given porphyrin molecule: $S_0 \rightarrow S_1$ and $S_0 \rightarrow S_2$ transitions in the visible range (giving rise to two Q-bands) and $S_0 \rightarrow S_3$ and $S_0 \rightarrow S_4$ transitions in the UV range (giving rise to the Soret B-band due to smaller energy splitting between them). Experimentally observed four bands in the visible range for the free base porphyrins are due to the equidistant vibrational progression with vibrational spacing Δν belonging to each of two Q-bands. The vibrational spacing Δν can be derived from the analysis of the fluorescence spectra.

According to the results of quantum-chemical calculations,[6,13-15,21] the relative positions of the four orbitals in the free base corroles differ strongly compared to the free base porphyrin with the same architecture of peripheral substitution (Figure 2).

Two lowest unoccupied molecular orbitals LUMO (c_1) and LUMO+1 (c_2) is known to degenerate in the porphyrin macrocycles which substituted with aryl groups in the C_m-positions. The highest occupied molecular orbital HOMO (b_1) energy increases due to the donation of the electron density from aryl substituents, whereas HOMO–1 (b_2) position remains unchanged since it has nodes at the C_m-positions. On the contrary, according to the quantum-chemical calculations,[6,13-15,21] in the free base corrole macrocycle LUMO and LUMO+1 orbitals do not degenerate, the energy difference Δ*E*(LUMO+1 – LUMO) is even higher than Δ*E*(HOMO – HOMO–1) gap (Figure 2). It was shown, in going for the T1 to T2 tautomer the Δ*E*(HOMO – HOMO–1) gap barely increases due to decrease in energy of HOMO-1 (b_2) orbital, and at the same time the Δ*E*(LUMO+1 – LUMO) gap increases noticeably due to increase in energy of LUMO+1 (c_2).[6,15] The orbital origin for each of four molecular orbitals does not change

upon NH-tautomerization. Analysis enabled authors to identify the individual spectra of the T1 and T2 tautomers of the 10-(4,6-dichloropyrimidinyl)-5,15-dimesitylcorrole H_3PMes_2Cor, bearing the substituents in C_m-positions (Figure 3).

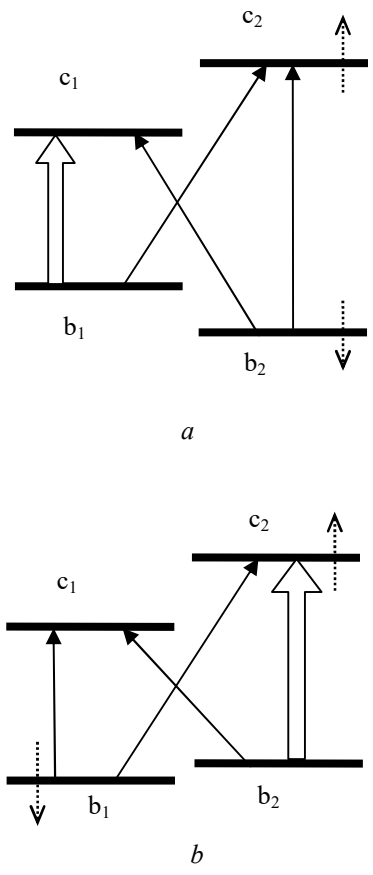

Figure 2. Schematic molecular orbitals diagram for: a) T1 tautomer of the C_m-substituted corrole; b) T1 tautomer of the C_b-substituted corrole. Dotted arrows indicate the direction of LUMO+1 and HOMO-1 shifts in going from T1 to T2 tautomer.[6,21]

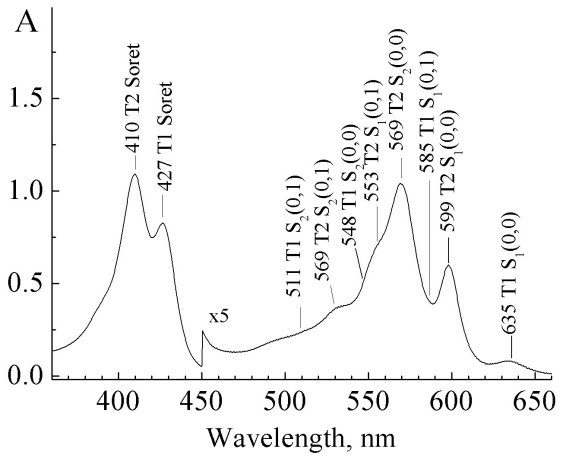

Figure 3. Assignment of the bands in the absorption spectrum of the 10-(4,6-dichloropyrimidinyl)-5,15-dimesitylcorrole H_3PMes_2Cor to the transitions belonging to individual NH-tautomers.[6] The absorbance in the 450–660 nm range has been multiplied by factor 5 for sake of clarity.

Later the same approach has been applied to make the transitions assignment in absorption spectra of the 2,3,7,13,17,18-hexamethyl-8,12-di-*n*-butylcorrole and 7,13-dimethyl-8,12-di-*n*-butylcorrole, bearing the substituents in C_b-positions (Figure 4).[21] A comparison of bands assignment in the electronic absorption spectra of C_b-substituted alkylated corrole free bases and C_m-substituted aryl derivatives led to the conclusion that ordering of the electronic states were different in these corrole derivatives.[6,21] The second excited singlet S_2 state of the long-wavelength tautomer Tl of $H_3OAlkCor$ and $H_3TAlkCor$ was lower in energy compared to the S_2 state of the short-wavelength tautomer T2 while the opposite pattern was observed for the C_m-substituted aryl derivatives, *i.e.*, the S_2 state of tautomer T2 lies lower than that of tautomer T1. This was a direct consequence of the two highest occupied molecular orbitals (HOMOs) being inverted depending on the architecture of the peripheral substitution on the corrole macrocycles. The HOMO was $b_1(a_{2u})$-like for C_m-substitution and $b_2(a_{1u})$-like for C_b-substitution while the HOMO–1 was $b_1(a_{2u})$-like for C_b-substitution and $b_2(a_{1u})$-like for C_m-substitution.

The C_b-substitution architecture with alkyl groups has been proposed to have a significant effect on the molecular conformation of the shortened corrole macrocycle. In contrast to C_b-alkylated porphyrins, in which steric interactions of substituents are localized on the individual pyrrole rings, the reduction in the distance between the carbon atoms C_2 and C_{18} in the dipyrrole fragment of the corrole macrocycle leads to the fact that, upon the introduction of substituents at these positions their Van der Waals spheres may overlap, and the "sterically perturbed" region extends over two adjacent pyrrole rings (Figure 5).

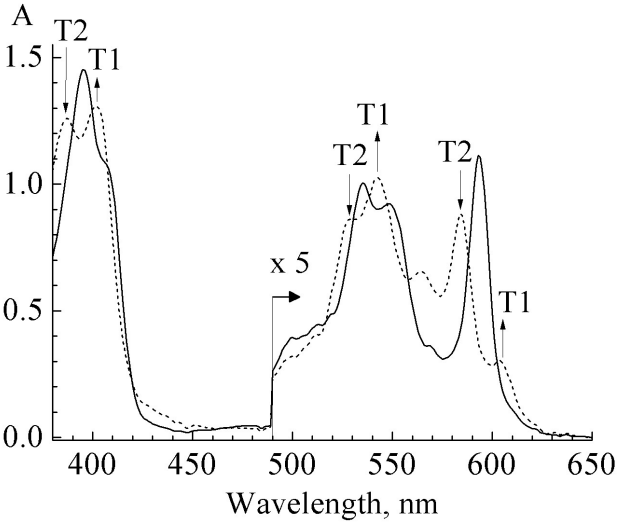

Figure 4. Ground state absorption spectra of the $H_3TAlkCor$ (dotted line) and the $H_3OAlkCor$ (solid line) in DCM at 293 K.[8] The absorbance in the 490 – 650 nm range has been multiplied by factor 5 for sake of clarity. The arrows indicate the direction of spectral changes in the spectrum of the H_3TAlkC due to increased proportion of the T1 tautomer formed at the expense of the T2 tautomer. The T1 tautomer absorption bands of the $H_3OAlkCor$ are barely visible, and the T2 tautomer absorption dominates.

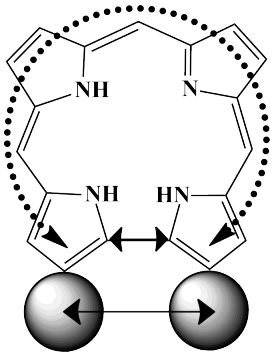

Figure 5. Schematic representation of sterical interactions between substituents in C_2 and C_{18} positions of dipyrrole fragment and its influence on the C_1–C_{19} bond length.[6,21]

The C_1–C_{19} bond length decreases if these positions are not substituted, the size of the macrocycle core decreases, and prerequisites for non-planar distortions are created. On the contrary, steric interactions of substituents at the C_2 and C_{18} positions lead to an increase in the C_1–C_{19} bond length and, accordingly, to the planarization of the macrocycle. The above-mentioned H_3TAlkCor belongs to the first case, and H_3OAlkCor belongs to the second one. Since the electronic effects of *n*-alkyl substituents are weak, it was assumed that these structural differences in the C_b-derivatives make the main contribution to the observed peculiarities in the spectral-luminescent and photophysical characteristics found for the tetra- and octa-substituted free base corroles: the efficient NH-tautomerization in the lowest excited singlet S_1 state was found for the H_3TAlkCor but there was no evidences of the tautomerization for the H_3OAlkCor.[21]

One can point out one more distinct difference of the absorption spectra of the free base corroles and porphyrins. The first one consists in smaller difference in the extinction coefficient between the Q-bands and Soret band in corroles. It is likely to be the result of the shifts of HOMO and LUMO orbitals compared to the porphyrin. Indeed, both dihydro- and tetrahydroporphyrins have similar arrangement of HOMO and LUMO orbitals and reveal the same trend in the absorptivity of bands.

The macrocycle of the free-base corroles is significantly more acidic than the macrocycle of porphyrins.[2,24] This favors dissociation of the pyrrole protons and creates prerequisites for formation of the deprotonated form.[2,5,24-25] The molecular structures of the deprotonated form of corroles and the products formed upon dissolution of the free base corroles in polar (electron-donating) aprotic solvents were convincingly proven to be identical by spectroscopic methods.[5,26-28]

In Figure 6, the gradual transformation of the free base corrole (in EtOH) to deprotonated form (in MeCN) is shown upon change in the proportion of two solvents in the binary mixtures.[5] Trace amounts of water in the aprotic solvents such as MeCN or DMF was found to promote the shift of the equilibrium between deprotonated form and the free base corrole in the direction of latter.[5]

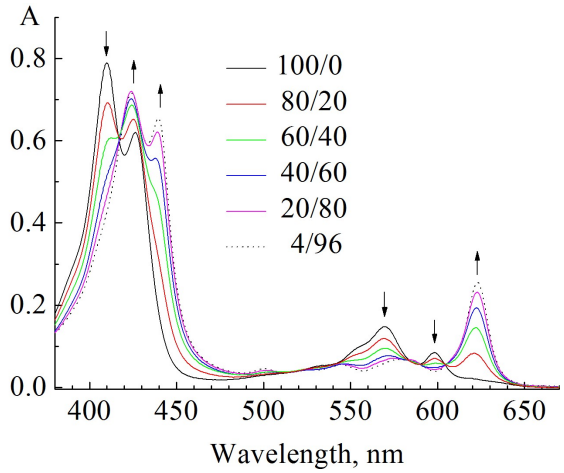

Figure 6. Ground state absorption spectra of the 10-(4,6-dichloropyrimidinyl)-5,15-dimesitylcorrole H_3PMes_2Cor in binary EtOH/MeCN mixtures (vol.%).[5]

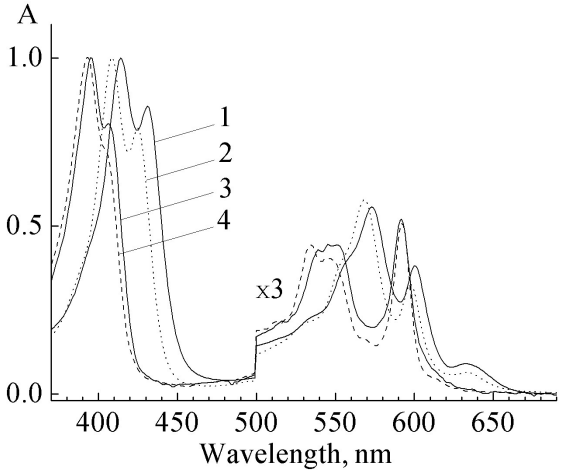

Figure 7. Ground state absorption spectra of the 10-(4,6-dichloropyrimidinyl)-5,15-dimesitylcorrole H_3PMes_2Cor in pyridine (1) and methanol (2); the 2,3,7,13,17,18-hexamethyl-8,12-di-*n*-butylcorrole H_3OAlkCor in ethanol (3) and dichloromethane (4).[29] Spectra in each pair were normalized on the maximum of the *B* band (Soret) of T2 tautomer. The absorbance in the 500 – 690 nm range has been multiplied by factor 3 for sake of clarity.

Solvatochromism of two free base corroles (Figure 7) with different architecture of peripheral substitution in a series of solvents of different nature has been studied.[29] The nature of the solvatochromic effects is analyzed by the Valentine method,[30] where as a measure of the solvation ability of solvent the function the solvent refraction index $f(n) = (n^2 - 1)/(2n^2 + 1)$ has been taken []. The function quantifies the general solvent effects upon solvation arising due to electron density redistribution in the solvent molecules.[31] The Valentine method has been used successfully to distinguish between general and specific solvent effects in the solutions of the 5,10,15,20-tetraphenylporphyrin free base and its zinc complex, and the dodecaphenylporphyrin free base.[30,32] Linear dependence of the spectral shift versus $f(n)$ indicates the absence of specific effects upon solvation in given solvents.

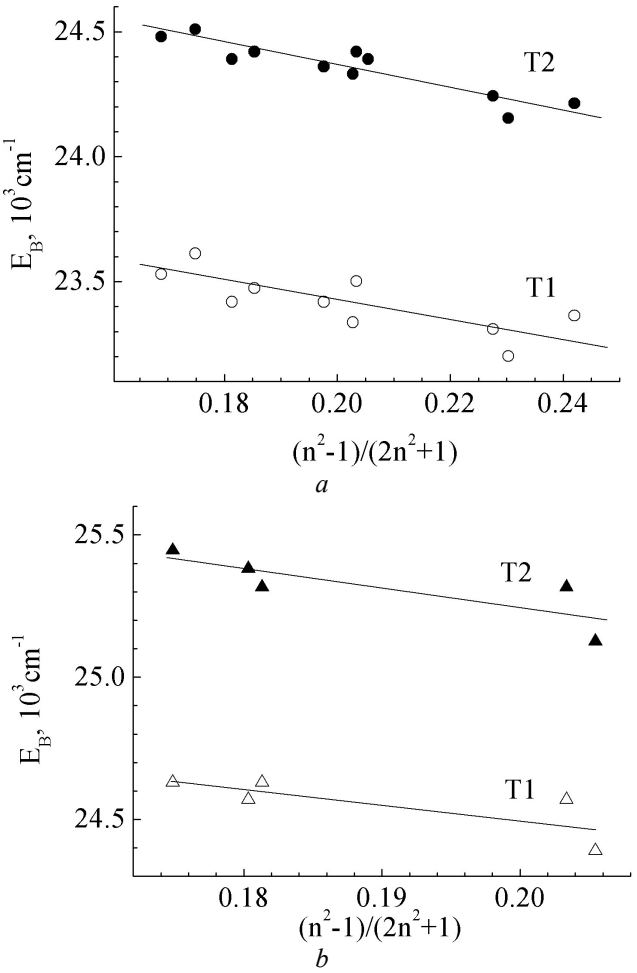

Figure 8. The *B*-band maximum plotted versus the solvent refraction index function $f(n) = (n^2 - 1)/(2n^2 + 1)$ for two NH tautomers of: a) H_3PMes_2Cor; b) $H_3OAlkCor$. Lines are the linear regressions as described in text.[29]

The dependences were satisfactorily approximated by the linear function $E_B = af(n) + b$, where the slopes *a* were different for the two tautomers, namely – 4040 cm^{-1} for the T1 tautomer and – 4550 cm^{-1} for the T2 tautomer (Figure 8a). The short-wavelength T2 tautomer of the $H_3OAlkCor$ is also solvated stronger compared to the long-wavelength T1 tautomer. The slope *a* of linear regression for the T1 tautomer is –5270 cm^{-1}, whereas for the T2 tautomer it goes up to –6800 cm^{-1} (Figure 8b). Thus, the spectral shifts of the absorption bands of NH tautomers of the H_3PMes_2Cor and $H_3OAlkCor$ are explained by nonspecific solvation general nonspecific interactions, and the short-wavelength T2 tautomer experiences stronger solvation in both cases. It was suggested that stronger solvation of the T2 tautomer bring to its domination in the solution.

In polar aprotic solvents (acetone, acetonitrile, dimethylformamide, and dimethylsulfoxide), specific acid-base interactions occur simultaneously with general solvent effects, leading to the formation of the deprotonated form.[5,28-29,33] Such specific interactions are stronger for the C_m-substituted corroles compared with C_b-substituted ones, due to their higher acidity.

The steric interactions of the three protons in the macrocycle core of free-base corroles are able to cause the nonplanar conformers even without steric strain on the macrocycle periphery, and the formation of nonplanar conformers is known to induce the shifts and broadening of bands in absorption spectra of tetrapyrrolic compounds.[34-35] This factor plays synergistically together with combined C_b- and C_m-substitution giving rise to huge nonplanar distortion clearly visible in the batochromic shift of spectrum.[4,34,36]

The significant nonplanar distortions of the macrocycle, which result in the pyrrole and pyrrolenine ring *N* atoms being exposed in solution,[37] create the conditions for specific solvation of the macrocycle core, primarily formation of intermolecular H-bonds with solvent molecules. The significant pyramidal nature of the pyrrole ring *N* atoms facilitates this,[3,6,37] because the manifestation (increase) of pyramidal nature is proportional to the increased acidity of the pyrrole ring and the macrocycle in general.[37] Because the molecular orbitals involved in electronic transitions in the visible and UV spectral regions have nonzero electron density on the nitrogens of pyrrole rings, the involvement of the latter in specific intermolecular interactions can markedly affect the spectral and photophysical properties of the free base corroles.[28,29,32]

Peculiarities of Excitation Energy Deactivation in the Free Base Corroles

The excited state properties of the free base corroles are similar to those of the free base porphyrins, but the differences in the molecular and electronic structure bring new specific features. *First of all*, due to coexistence of NH-tautomers all the photophysical parameters found for the free base corrole solutions should be treated as variables, depending on the given proportion of NH-tautomers, if only they are not related to one of them. In addition, the NH-tautomerization in the lowest excited singlet S_1 state was found to take place with high efficiency.[16] The excitation energy deactivation pathways analysis in the free base 10-(4,6-dichloropyrimidinyl)-5,15-dimesityl-corrole demonstrate that NH-tautomerization in the lowest singlet S_1 state of the T2 tautomer is able to compete with the intersystem $S_1 \rightarrow T_1$ crossing. Due to activation character of the NH-tautomerization in the lowest singlet S_1 state with activation energy E_a lying in the range of 1–5 kcal/mol, the rate constant of NH-tautomerization increases dramatically with the temperature rise: from $1.48.10^9$ s^{-1} at 293 K up to $2.78.10^9$ s^{-1} at 318 K.[38] Therefore with temperature increase T2→T1 NH-tautomerization becomes the dominant process of the deactivation of the short-wavelength T1 tautomer, and, after phototautomerization almost 90% of the electronic excitation energy of an ensemble of the 10-(4,6-dichloropyrimidinyl)-5,15-dimesityl-corrole in solution is accumulated on the lowest excited singlet S_1 state of the long-wavelength T1 tautomer at a temperature of 318 K (Figure 9). Thus, *the second* feature is that NH-tautomerization in the lowest excited singlet S_1 state of the short-wavelength T2 tautomer causes significant temperature dependence in the quantum yields of deactivation pathways of its excitation energy (Figure 10).[16,38]

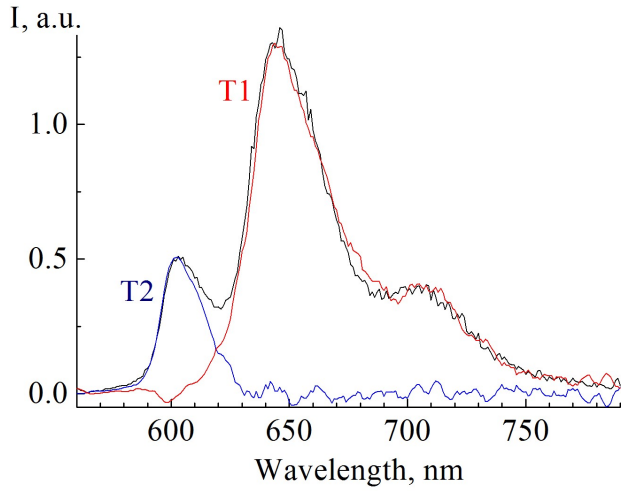

Figure 9. Fluorescence spectra of the 10-(4,6-dichloro-pyrimidinyl)-5,15-dimesitylcorrole in EtOH (black line), and its decomposition to the individual spectra of T1 (blue line) and T2 (red line) tautomers.[16]

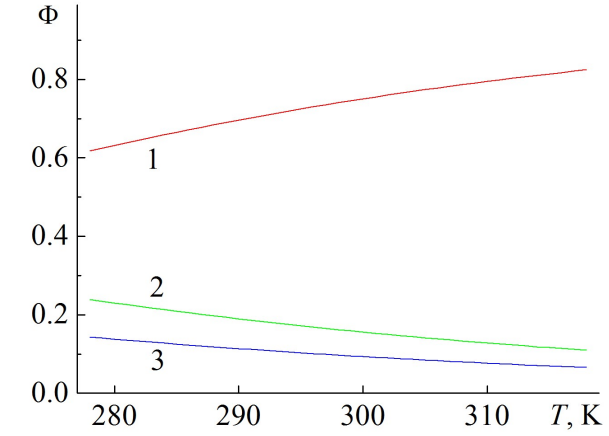

Figure 10. Quantum yields of deactivation channels of lowest excited singlet S_1 state of the T2 tautomer of the H_3PMes_2Cor as a function of temperature: 1 – NH-tautomerization, Φ_{NH}; 2 – intersystem crossing, Φ_{ISC}; 3 – fluorescence, Φ_{fl}.[38]

As a result of the NH-tautomerization in the lowest excited singlet S_1 state the shape of the fluorescence spectrum changes. Increase in the contribution of the short-wavelength T2 tautomer takes place not only with the temperature rise, but also due to changes in the architecture of peripheral substitution (Figure 11), or isotopic H-D exchange in the macrocycle core (Figure 12). In all these cases the increase in its intensity takes place at the expense of the emission band of T1 tautomer.

The main channel of the excited singlet S_1 state deactivation the long-wavelength T1 tautomer of the free base corroles is the $S_1 \rightarrow T_1$ intersystem crossing. This statement is also valid for the T2 tautomer at low temperatures and in conditions where the NH-tautomerization is prohibited. Direct phosphorescence measurements for the series of the C_m-substituted free base corroles have revealed that the energy gap $\Delta E(S_1–T_1)$ in the T2 tautomer (this tautomer dominates at low temperatures, which need to observe phosphorescence) of all studied molecules had unusually large value amounting of 5300–5500 cm^{-1}.[39] Surprisingly, this value is much higher than the corresponding value for the corrole metallomplexes amounting of up to 4000 cm^{-1}.[40-43] In case of porphyrins the $\Delta E(S_1–T_1)$ gap value is known to depend on both the substitution pattern and the degree of nonplanar macrocycle distortions, with the highest value of about 4800 cm^{-1} has been reported for the doubly protonated form of the 5,10,15,20-tetraphenylporphyrin.[35,44] It was expected that such a high energy gap $\Delta E(S_1–T_1)$ values originate due to lifting of the LUMO and LUMO+1 orbital degeneracy, which, in its own turn, influences the configuration interaction in the triplet state in such a specific manner.[39] Recent communication about the $\Delta E(S_1–T_1)$ value of the same order of magnitude for the deprotonated corrole whose macrocycle is known to be planar, excludes any possibility to account for large $\Delta E(S_1–T_1)$ value by intrinsically nonplanar conformation of the free base corroles macrocycle.[33]

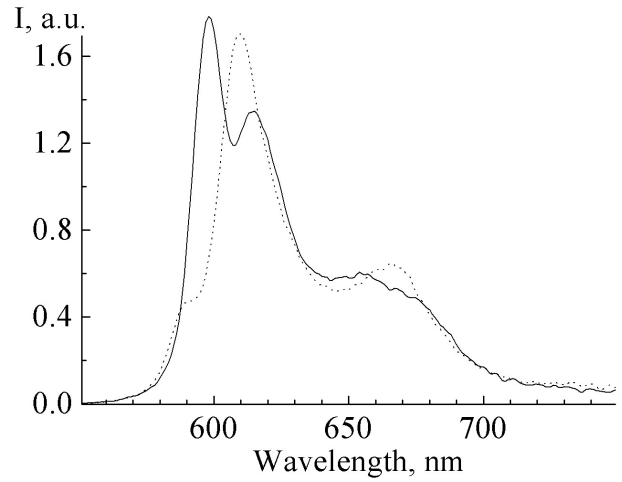

Figure 11. Fluorescence spectra of the 2,3,7,13,17,18-hexamethyl-8,12-di-*n*-butylcorrole $H_3OAlkCor$ (solid line) and the 7,13-dimethyl-8,12-di-*n*-butylcorrole $H_3TAlkCor$ (dashed line) in dichloromethane at 293 K.[21]

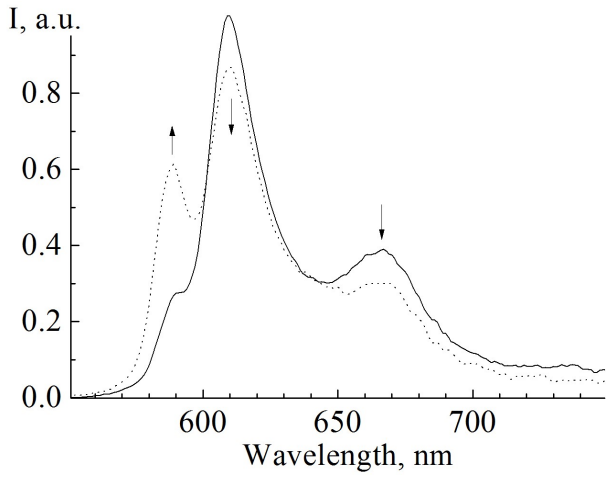

Figure 12. Fluorescence spectra of the 7,13-dimethyl-8,12-di-*n*-butylcorrole $H_3TAlkCor$ in dichloromethane (solid line) and after addition of two drops of EtOD (dotted line) at 293 K. Arrows indicate the direction of spectral changes upon deuteration.[21]

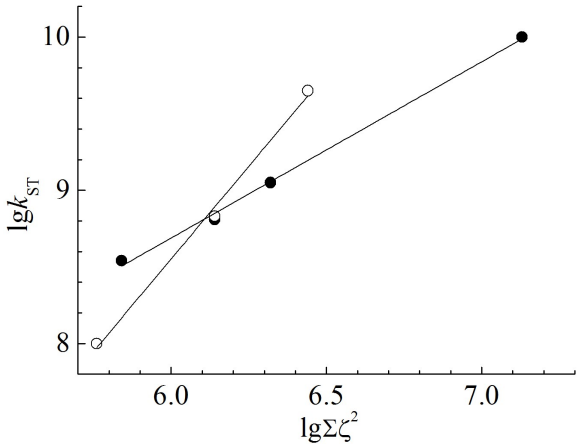

Figure 13. Dependence of the the $S_1 \rightarrow T_1$ intersystem crossing rate constant k_{ISC} on the sum of the spin-orbit coupling constants squared $\Sigma\zeta^2$ of *ortho*-halogens in C_m-aryl groups of free base porphyrins (open circles) and corroles (closed circles) in double logarithmic coordinates. Lines represent least-square linear regressions.[50]

We think the large $\Delta E(S_1–T_1)$ gap to be *the third* specific factor influencing the excited states deactivation in free base corroles. Indeed, the intersystem crossing rate constant k_{ISC} is inversely proportional to the $\Delta E(S_1–T_1)$ value.[45] Decrease in the k_{ISC} value enables the fluorescence rate constant k_{fl} to compete. As a result, the reported to date fluorescence quantum yields are systematically larger compared to porphyrins with similar substitution pattern.[46-49] The spin-orbit interactions caused by the attachment of aryl groups with *ortho*-substituted halogen atoms to the C_m-positions of the tetrapyrrolic macrocycle of the free base corroles and porphyrins have been studied recently.[50] The relationship between the intersystem crossing rate constant k_{ST} and the sum of the spin-orbit coupling constants squared $\Sigma\zeta^2$ of halogen atoms was analyzed (Figure 13). The slope a of dependence $\lg k_{ST} = a\lg\Sigma\zeta^2 + b$ is for 2,1 times higher for the studied free base porphyrins series compared to that for the corroles series. It was concluded that the internal heavy atom effect, caused by halogen atoms, in porphyrins led to two-fold increase in the rate of the intersystem crossing growth as compared to corroles. It is proposed that this is due to significant differences in the energy gap between the lowest excited singlet S_1 and triplet T_1 states $\Delta E(S_1–T_1)$ between corroles and porphyrins. Therefore, one can state that the internal heavy atom effect on the $S_1 \rightarrow T_1$ transition in the corrole macrocycles is weaker compared to that in the porphyrins. This feature makes corroles attractive from point of view of design of dual emitters, since the fluorescence is not quenched when the phosphorescence appears, and two emissions have comparable quantum yields.

Fluorescence of Free Base Corroles

Under excitation into any of Q- or B-bands the free base corroles reveal the fluorescence with the structured spectrum and the lifetime in the nanosecond range.[5-6,15-16,18,24,48-49,51-54] The fluorescence quantum yield Φ_{fl} was found to be of the same order of magnitude or even higher as it was in the free base porphyrins. The fluorescence spectra have been measured for practically all new free base corrole derivatives prepared, but the detailed analysis of fluorescence properties has not been carried out. Most of the studied compounds were corrole derivatives substituted in the C_m-positions with different aryl groups,[18,48-49,51,55] and much less of papers dealt with the alkylated derivatives substituted in the C_b-positions or those having mixed $C_m + C_b$ architecture of substitution.[15,51,54] It should be stressed that taking into account NH-tautomerization and, especially, easy formation of deprotonated species in polar aprotic solvents, all the early data should be analyzed with care.

The most reliable considerations can be done for the 5,10,15-triaryl-corrole family (see Table 1) which can be divided into two structural groups with or without the sterical hindrances for the aryl rings rotation. Nevertheless, as one can see from the data presented in Table 1, there are no noticeable differences for the representatives of these two groups. Both of them have the fluorescence quantum yield order of 0.20, and barely depend on the structure of the aryl groups. The Φ_{fl} values in Table 1 are mutually consistent between the reports from different groups. It is worth to point out, that these derivatives have the substitution patterns of AB_2 and A_3 type.

The decrease in the Φ_{fl} value found for the derivatives having high loading of macrocycle (or C_m- aryl substituents) with halogens should be commented separately. The fluorescence quenching should be related to the enhancement of the spin-orbit coupling (SOC) due to heavy atom effect. Thus, the spin-orbit coupling constant values ζ of F, Cl, Br and I are 269, 587, 2460 and 5069 cm^{-1}.[56] As the rate of spin-orbit coupling depends on the sum of squared ζ values, the overall influence will be sufficiently large even for the fluorine substituted derivatives. Higher Φ_{fl} values reported for the derivatives with fluorine substitution at *meta*- or *para*-positions of aryl rings compared with those at *ortho*-positions, are in line with observation made for the porphyrin derivatives,[57-58] that spin-orbit coupling differs for *ortho*-, *meta*- and *para*-positions of aryl ring, with that for the substitution in the *ortho*-positions has the highest one. Thus, the fluorescence quenching should be stronger in such a case. In previous section we have stressed, that heavy atom effects are weaker than in the porphyrins due to larger energy gap between S_1 and T_1 states in the free base corroles.[39,50]

The fluorescence quantum yield Φ_{fl} value for the 2,3,7,8,12,13,17,18-octaalkyl-corrole derivatives was found to be of the same order of magnitude. Introduction of the electron-withdrawing NO_2 group into one of the C_b positions or in the aryl ring was found to lead to the pronounced fluorescence quenching by the charge-transfer mechanism.[49,51,54] It is worth to point out that the solvent dependence of the fluorescence quantum yield Φ_{fl} has been observed for the 2,3,7,13,17,18-hexamethyl-8,12-di-*n*-butylcorrole H_3OAlkCor.[59] The observed differences have been assigned to the solvent induced shifts in the NH-tautomeric equilibrium in the excited S_1 state. It was suggested that activation barrier for NH-tautomerization is modulated by solvation shell. In protic solvents, the barrier height is lower, and in aprotic it goes up.

The derivative with mixed C_m + C_b architecture of substitution revealed the huge decrease in the Φ_{fl} value down to $6 \cdot 10^{-5}$ without the substitution with heavy atoms.[51] By analogy with polysubstituted sterically hindered porphyrins one can suggest an increase in the radiationless deactivation rate k_d in such a case due to macrocycle deformation and promotion of the fast radiationless decay of the S_1 state. Here it is a case, since the phenyl ring attached to the carbon C_{10} of macrocycle has hindered contacts with two neighboring alkyl groups attached at C_8 and C_{12} positions of adjacent pyrrole rings.

An extension of the number of available free base corrole derivatives enabled to verify and go further in the revealing relationships between the molecular structure and fluorescent properties of the lowest excited S_1 state. Thus, in case the aryl rings bearing bulky groups in their *ortho*-positions, the aryl planes keep in the almost perpendicular positions to the neighboring fragment of the macrocycle, and the rigid molecular conformers form which are revealed by narrowing of the bands in the absorption and fluorescence spectra. The radiationsless deactivation in these conformers decreases and higher fluorescence quantum yield Φ_{fl} value are expected.[53]

The signatures of the spin-orbit coupling has been proved with a large set of 5,10,15-triarylcorroles of AB_2, BA_2 and A_3 types of C_m-substitution with aryl groups bearing the fluorine, chlorine and bromine atoms in the *ortho*-positions.[49] The phosphorescence spectra have been measured for these compounds at 77 K due to enhancement of both the $S_1 \rightarrow T_1$ and $T_1 \rightarrow S_0$ intersystem crossing rates.[39]

Table 1. The photophysical properties of selected free base corroles*.

No.	Corrole	Solvent	$\Phi_{fl} \cdot 10^2$	τ_{fl}, ns	k_{fl}, 10^7, s^{-1}	Φ_{ISC}/Φ_{Δ}	Ref.
1	5,10,15-tris-phenylcorrole	toluene	21/16	4.8	4.4/3.5	–/0.51	[48]
2	5,15-dimesityl-10-(4-CN-phenyl)corrole	toluene	18.0	6.3	2.9	–/0.52	[48]
3	5,10,15-tris(4-CF_3-phenyl)corrole	toluene	20.0	5.2	3.9	–/0.61	[48]
4	5,10,15-tris(3,5-di-CF_3-phenyl)corrole	toluene	20.0	5.7	3.5	–/0.64	[48]
5	5,15-di-C_6F_5-10-tolylcorrole	toluene	14.0	4.1	3.4	–/0.77	[48]
6	5,10,15-tris-C_6F_5-corrole	toluene /DCM	13/6	4.8	2.7	0.72/ 0.71	[48]/ [55]
7	10-(4,6-di-Cl-pyrimidinyl)-5,15-dimesitylcorrole	toluene	6.0	2.3	2.6	0.85/–	[39]
8	10-phenyl-5,15-(4,6-di-Cl-pyrimidinyl)corrole	toluene	4.6	1.4	3.3	0.90/–	[39]
9	5,10,15-tris(4,6-di-Cl-2-sylfomethylpyrimidinyl)corrole	toluene	2.5	0.85	2.9	0.94/–	[39]
10	10-(4,6-di-Br-pyrimidinyl)-5,15-di-(4,6-di-Cl-2-sylfomethyl-pyrimidinyl)corrole	toluene	0.45	0.1	4.5	0.99/–	[39]
11	2,3,7,8,12,13,17,18-octamethylcorrole	MeTHF	7.0	7.5	0.93	–/–	[54]
12	2,3,7,8,12,13,17,18-octamethyl-5-phenylcorrole	MeTHF	0.05	<0.4	>0.13	–/–	[54]
13	2,3,7,8,12,13,17,18-octamethyl-5,10,15-triphenylcorrole	toluene	0.006	<0.5	>0.012	–/–	[51]
14	5,10,15-tri(3-NO_2-phenyl)corrole	toluene	8.2	5.2	1.6	–/–	[51]
15	5,10,15-tri(4-NO_2-phenyl)corrole	toluene	9.5	5.7	1.7	–/–	[51]
16	10-(methoxycarbonylphenyl)-5,15-di-C_6F_5-corrole	toluene	15.0	4.1	3.7	–/–	[15]
17	2,3-di-Br-10-(methoxycarbonylphenyl)-5,15-di-C_6F_5-corrole	toluene	1.1	0.24	4.6	–/–	[15]
18	2,3,17-tri-Br-10-(methoxycarbonylphenyl)-5,15-di-C_6F_5-corrole	toluene	0.51	0.12	4.3	–/–	[15]
19	2,3,17,18-tetra-Br-10-(methoxycarbonylphenyl)-5,15-di-C_6F_5-corrole	toluene	0.47	0.084	5.6	–/–	[15]
20	10-(4,6-di-Cl-pyrimidinyl)-5,15-di(2,6-di-Cl-phenyl)corrole	DCM	2.0	0.8	2.5	–/–	[49]
21	10-(4-NO_2-phenyl)-5,15-di-(4,6-di-Cl-2-sylfomethyl-pyrimidinyl)corrole	DCM	1.1	0.42	2.6	–/–	[49]
22	10-(4-Cl-phenyl)-5,15-di-(4,6-di-Cl-2-sylfomethyl-pyrimidinyl)corrole	DCM	3.6	1.42	2.5	–/–	[49]
23	2,3,17,18-tetra-I-5,10,15-triphenylcorrole	DCM	<0.09	–	–	–/0.97	[60]
24	5,15-di-C_6F_5-corrole	DCM	8.5	–	–	–	[61]
25	5,10-di-C_6F_5-corrole	DCM	7.7	–	–	–	[61]
26	10-NO_2-5,15-di-C_6F_5-corrole	DCM	<1	–	–	–	[62]
27	5,10-di-C_6F_5-15-2,6-di-Cl-phenylcorrole	DCM	5.9	–	–	–	[63]
28	5,10-di-C_6F_5-15-mesitylcorrole	DCM	9.9	–	–	–	[63]

Continuation of the **Table 1**.

29	5,10-di-C_6F_5-15-(4-NO_2-phenyl)corrole	DCM	4.0	–	–	–	[63]
30	5,10-di-C_6F_5-15-(2,4,5-trimethoxyphenyl)corrole	DCM	9.2	–	–	–	[63]
31	5,10-di-C_6F_5-15-naphthylcorrole	DCM	9.4	–	–	–	[63]
32	5,10-di-C_6F_5-15-(4,6-di-Cl-pyrimidinyl)corrole	DCM	4.1	–	–	–	[63]
33	5,15-di(2,3,5,6-tetra-F-4-methoxyphenyl)corrole	DCM	9.2	–	–	–	[64]
34	10-Cl-5,15-di(2,3,5,6-tetra-F-4-methoxyphenyl)corrole	DCM	2.3	–	–	–	[64]
35	10-phenylamino-5,15-di-(2,3,5,6-tetra-F-4-methoxyphenyl)corrole	DCM	10.4	–	–	–	[64]
36	10-carbazolyl-5,15-di(2,3,5,6-tetra-F-4-methoxyphenyl)corrole	DCM	9.2	–	–	–	[64]
37	10-C_6F_5-5,15-di(diethoxycarbonyl)corrole	DCM	16.5	4.13	4.0	–	[55]
38	5,15-di(diethoxycarbonyl)corrole	DCM	11.0	2.44	4.5	–	[55]
39	10-(4-NO_2-phenyl)-5,15-di(diethoxycarbonyl)corrole	DCM	17.0	3.01	5.6	–	[55]
40	10-(4-OH-phenyl)-5,15-di(diethoxycarbonyl)corrole	DCM	16.0	3.92	4.1	–	[55]
41	10-($C_{12}H_{25}$)-5,15-di(diethoxycarbonyl)corrole	DCM	17.5	3.02	5.8	–	[55]
42	10-($C_{16}H_{33}$)-5,15-di(diethoxycarbonyl)corrole	DCM	16.0	3.02	5.3	–	[55]
43	7,13-dimethyl-8,12-di-*n*-butylcorrole	DCM	12.0	–	–	–	[21]
		EtOH	5.9	–	–	–	[21]
44	2,3,7,13,17,18-hexamethyl-8,12-di-*n*-butyl-corrole	DCM	14.0	–	–	–	[59]
		MeCN	12.0	–	–	–	[59]
		DMF	14.2	–	–	–	[59]
		EtOH	8.3	–	–	–	[59]
		acetone	15.3	–	–	–	[59]
45	10-(4,6-diphenyl-pyrimidinyl)-5,15-(4,6-di-Cl-pyrimidinyl)corrole	DCM	10.0	4.32	2.31	–	[53, 65]

*The photophysical properties for the series of AB_2, BA_2 and A_3 types of C_m-substituted free base corroles are reported (32 molecules in total).[49,53,55,65] Part of them have barely distinguished photophysical properties due to similar structure of substituents. Therefore, one-two typical representatives have been included in the Table 1.

The correlations of changes in the radiationless deactivation rate k_d and fluorescence quantum yield Φ_{fl} from one side, and the $\Sigma\zeta^2$ value of chlorine atoms, from the other, unambiguously demonstrated that the heavy atom effect leads to the quenching, and also promotes the intersystem crossing.[39,49] This concept has been developed later for the free base (and metallated) corroles.[15,60,66] When number of bromine or iodine atoms attached to the C_b-positions of the pyrrole rings *A* and *D* increases, the gradual quenching of the fluorescence has been observed. In case of metallated derivatives the intensity of the $T_1 \rightarrow S_0$ phosphorescence increases simultaneously giving rise to dual emission at room temperature. The proportion of the fluorescence and phosphorescence can be finely tuned with temperature enabling to design molecular luminescent thermometer.[66]

Asymmetric 5,10-substitution compared to the symmetric 5,15-substitution was found do not bring specific features into the deactivation rates.[61] Structural factors could be expected here, since in case of the 5,10-substitution formally four NH-tautomers coexist. But in the first approximation there is no strong structural effects and the observed differences can be rationalized in terms of the variation of electronic effects of substitution (see Table 1).

The fluorescence spectrum profile consists of two distinct bands as in the free base porphyrins, but for numerous free base corrole derivatives the distinct third band appears in the spectrum, or it is clearly visible as a shoulder at the short-wavelength side of the 0-0 band (Figures 9,11,12). Its origin has been uncovered using the concept of coexistence of two NH-tautomers.[16] According to it, the measured fluorescence spectrum consists of the major contribution from one NH-tautomer (in the used terms, the long-wavelength T1 tautomer) and minor contribution of the second NH-tautomer (*i.e.* the short-wavelength T2 tautomer). The proportion of the emission from two NH-tautomers was shown to depend strongly on the temperature.[16] The influence of solvent on the tautomeric equilibrium has been also mentioned. The proportion between the individual emission spectra of two NH-tautomers was shown to change upon the deuteration on the macrocycle core.[16] Isotope D/H exchange in the pyrrole rings change dramatically the rate constant of NH-tautomerization, giving rise to increased proportion of the short-wavelength T2 tautomer emission. The slight increase in the fluorescence quantum yield has been reported upon deuteration of the free base corroles.

The total emission spectrum can be deconvoluted and the individual fluorescence spectra of NH-tautomers have been presented,[16] and their quantum yields have been measured. Thus, for example, the fluorescence quantum yield of the T1 tautomer of the 10-(4,6-dichloropyrimidinyl)-5,15-dimesitylcorrole was found to be 0.045, whereas the Φ_{fl} value for the T2 tautomer was as high as

0.155.[16] On the contrary, there were no difference in the fluorescence quantum yield Φ_{fl} values for two tautomers of the 7,13-dimethyl-8,12-di-*n*-butylcorrole H_3TAlkCor in dichloromethane solutions.[21] It seems that there is no general trend in this case. To date there were no reports on the differences in the fluorescence decay time for two NH-tautomers. It is not surprising, provided that efficient NH-tautomerization takes place in the lowest excited singlet S_1 state these figures should be practically indistinguishable.

Formation of deprotonated of monoprotonated products keeps the fluorescence properties of the corrole macrocycle.[5,24,53] It should be pointed out, that the formation of both monoprotonated and deprotonated molecules takes place with two distinct stages, reflecting their formation from two NH-tautomers with different rates.[17] However, being formed the unique species are observed. Observation of two states indicates that the rate of the protonation/deprotonation is faster compared to that of the NH-tautomerization. Temperature increases the NH-tautomerization rate and the formation of these species takes place with unique rate.[17] Each of these species has its own distinct fluorescence spectrum (Figure 14). The Stockes shift value has the same magnitude for all three species resulting in the same order of the bands as it holds for the absorption spectra. As for the fluorescence quantum yield Φ_{fl}, the highest value has been measured for the free bases. The Φ_{fl} value decreases slightly for the monoprotonated species. Concerning the Φ_{fl} value for the deprotonated corrole molecules both high and very low values have been reported.[5,53] The possible explanations lies in the different solvation of molecule in the aprotic and protic polar solvents and trace amounts of acids/bases. Specific solvation of the macrocycle core could take place, *i.e.* true deprotonation is observed in one case, when the H-bonded associates are formed in another one.[2,67] Since the vibrational modes of the core in tetrapyrrolic macrocycles participate in the radiationless deactivation of the excited states,[68] such a difference could contribute noticeably in the total rate of deactivation of the lowest excited S_1 state.

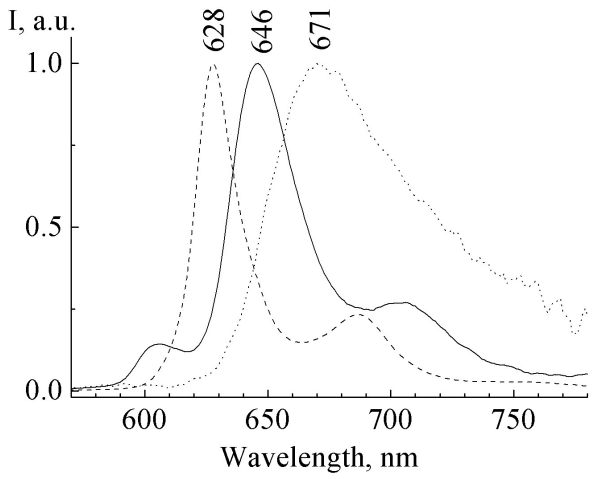

Figure 14. Fluorescence spectra of the 10-(4,6-dichloropyrimidinyl)-5,15-dimesitylcorrole free base H_3PMes_2Cor (solid line) and its deprotonated (dashed line) and monoprotonated (dotted line) forms at 298 K.[17]

Such a possibility has been studied using the sequential formation of protonated and deprotonated forms of the 2,3,7,13,17,18-hexamethyl-8,12-di-*n*-butyl-corrole in solution.[28] It was found that in the ground electronic state the spectral characteristics of each of the two forms are the same when they directly formed from the free base and from the antipodal form, while the fluorescence spectra of each of two forms differ depending on their formation way. It is proposed that there are specific interactions between the protonated and deprotonated forms of corroles in the lowest excited singlet S_1 state, due to the formation of a complex solvation shell which leads to hysteresis of the fluorescent characteristics of the protonated and deprotonated forms of corrole during their mutual transitions.

Properties of the Triplet States of the Free Base Corroles

There is limited information on the formation and deactivation of the lowest triplet T_1 state of the free base corroles compared to that on the lowest excited singlet S_1 state. There were few reports where these properties have been studied in detail.[39,48] The reason for this that triplet state intersystem crossing is expected to be noticeably higher for the metallated corroles rather than for the free bases, so the triplet state population for the possible applications would be higher in the former case. Thus, these circumstances reduce the interests to the triplet state studies for the free bases corroles.

As it has been shown in previous section, the intersystem crossing plays important role in the excitation energy deactivation of the free base corroles, and the intersystem crossing quantum yield Φ_{ISC} can be enhanced with appropriate substitution promoting the spin-orbit coupling. The efficient population is of interest from two points of view. First, quenching of the long-lived triplet T_1 states by molecular oxygen leads to the photosensitized formation of singlet molecular oxygen, which is a key agent in the photodynamic processes of Type II.[69] Second, triplet T_1 states are the source of the NIR phosphorescence that is of interest for the intracellular imaging and design of perspective organic phosphors. The applied works on the photosensitization with corroles are numerous (see review[70]), but these entire studies skip the detailed photophysical studies and limited in the most cases with measurements of the quantum yield of photosensitized formation of singlet oxygen Φ_{Δ}. It should be noticed that such measurements are much simpler to carry out compared the measurements of the intersystem crossing quantum yield. Since Φ_{Δ} value is the Φ_{ISC} product the probability of the singlet oxygen formation upon quenching of one molecule, the former value is often used as a lowest limit of Φ_{ISC} value.[69] Both values are identical in case when there is no competing (with quenching by molecular oxygen) deactivation processes.

The intersystem crossing Φ_{ISC} values of the free base corroles have been reported (see Table 1).[39,48] There was no relationship between the Φ_{ISC} (Φ_{Δ}) values with architecture of peripheral substitution. The only clearly observed trend was as increase in the intersystem crossing yield when macrocycle substituted with groups having (or

being themselves) heavy atoms such as halides. Thus, in going from the 5,10,15-tris-phenylcorrole to the 5,10,15-tris-pentafluorophenylcorrole the Φ_Δ value was found to increase from 0.51 to 0.71.[49] The Φ_{ISC} value for 5,10,15-triarylcorroles of AB_2, BA_2 and A_3 type (A is 4,6-dichloropyrimidinyl) increased from 0.85 to 0.94, and, when two chlorine atoms were replaced with bromine, amounted of 0.99.[39] The fluorescence has been strongly quenched in the last case, its quantum yield Φ_{fl} is $0.45.10^{-2}$ only.

Triplet state lifetimes lie in the range from about 50 to 150 microseconds, thus allowing the complete quenching of the T_1 states with molecular oxygen.[48] The bimolecular quenching rate constant k_q values are of the same order of magnitude as those for the free base porphyrins.[48,71] So far, there was no reported on the correlation between the rate constant k_q and oxidation potential of corrole macrocycle. One can suggest that in the early studies the confusion with assignment of the species to the free base took place and some of the figures have been taken for the deprotonated molecules.

The possibility of the radiative deactivation of the lowest triplet T_1 state of the free base corroles has been discussed repeatedly but, there were no reports on the phosphorescence measurements until recently,[39] in contrast with numerous phosphorescence observations in the metallocomplexes.[61-64 and Refs. therein] The $T_1 \rightarrow S_0$ emission has been measured for the first time at 77 K for the series of 5,10,15-triarylcorroles with different strength of the spin-orbit coupling due to multiple halide atoms attached to C_m-substituents (Figure 15). It was expected that quantum yield of the phosphorescence would enhance with increase in the sum of spin-orbit coupling constants squared $\Sigma\zeta^2$ value of halides. The experiment was found to be in the full agreement with these expectations. Thus, the phosphorescence quantum yield Φ_{ISC} value of $9.7.10^{-4}$ has been measured for the molecule with one 4,6-dichloropyrimidinyl group, whereas $\Phi_{ISC} = 1.7.10^{-3}$ has been obtained for the molecule with two 4,6-dichloropyrimidinyl and one 4,6-dibromopyrimidinyl groups.[39] For the latter derivative due to simultaneous quenching of the fluorescence quantum yield Φ_{fl} and enhancement of the phosphorescence quantum yield Φ_{ISC} both emissions have the intensity in the same range, *i.e.* dual emission with intensity in the same range is observed.

Triplet T_1 state lifetime at 77 K, measured with phosphorescence decay kinetics, decrease from 6.6 milliseconds down to 0.4 milliseconds in going from the 10-(4,6-dichloropyrimidinyl)-5,15-dimesitylcorrole to the 10-(4,6-dibromopyrimidinyl)-5,15-di-(4,6-dichloro-2-sulfomethyl-pyrimidinyl)corrole. This trend is reciprocal to that observed for the S_1 state lifetime, and it is consistent with the signature of the heavy atom effect. The reported phosphorescence data should be assigned to the short-wavelength T2 tautomer.[39] It is due to the absence of excited state NH-tautomerization in the S_1 excited state at 77 K,[16] as a result single species exist in solid solution at this temperature. In relation to this fact, it is worth to compare the value $\Phi_{ISC} = 0.72$ for the T2 tautomer of the 5,10,15-tris-C_6F_5-corrole at 77 K and $\Phi_\Delta = 0.71$ measured in the heterogeneous solution of the T1 and T2 tautomers at 298 K.[39,48] Practically the same figures allow suggesting that intersystem crossing quantum yield Φ_{ISC} in both NH-tautomers is the same within experimental error.

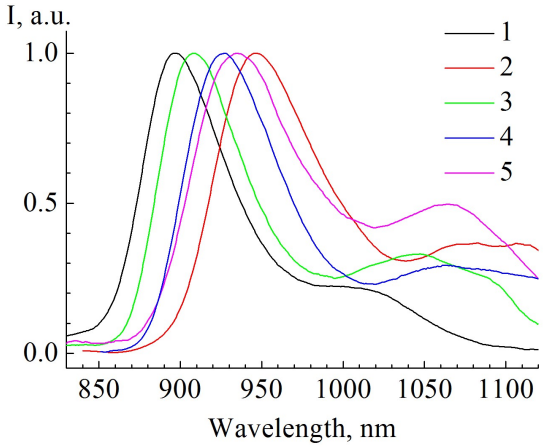

Figure 15. Normalized phosphorescence spectra of the free base corroles at 77 K in glassy mixture toluene : EtOD (10:1):
1 – 10-(4,6-di-Cl-pyrimidinyl)-5,15-dimesitylcorrole;
2 – 10-phenyl-5,15-(4,6-di-Cl-pyrimidinyl)corrole;
3 – 5,10,15-tris-(4,6-di-Cl-2-sylfomethylpyrimidinyl)corrole;
4 – 10-(4,6-di-Br-pyrimidinyl)-5,15-di-(4,6-di-Cl-2-sylfomethyl-pyrimidinyl)-corrole; 5 – 5,10,15-tris-C_6F_5-corrole.[39]

Conclusions

The free base corroles being structurally similar to the free base porphyrins but lacking of one methine bridge in the macrocycle reveal their own unique spectral-luminescent and photophysical properties. Due to macrocycle core rearrangement the NH-tautomeric forms coexist that results in the intrinsic heterogeneity of the free base corroles samples. Each of the NH tautomers has its own unique electronic density distribution and π-conjugation pathway. The NH tautomerization was shown to occur in both the ground and excited states. The ground state energies of NH-tautomers are similar and the tautomerization barrier is low leading to barely distinguished temperature dependence. On the contrary, the pronounced temperature dependences of the fluorescence spectra as well as the rates of the excitation energy deactivation have been reported with the NH-tautomerization rate constant in the lowest excited S_1 state being the dominate one. Overcrowding of three core protons leads to the formation of highly distorted macrocycle with pyrrole/pyrrolenine nitrogens being exposed to the solvent. Such structural changes are responsible for the pronounced general and specific solvation effects, which are able to promote the chemical alterations such as core protonation/deprotonation without any traces of acids or bases. Finally, macrocycle contraction leads to the lifting of degeneracy of two lowest unoccupied molecular orbitals. Increase in the energy spacing between them changes the interaction between two one-electron configurations reflected by the spectral changes. Changes of the molecular orbitals energies lead to huge increase in the S_1–T_1 energy gap, which, in its own turn, modulates the spin-orbit coupling strength and the competition between all the rates of the lowest S_1 excited state deactivation. Beside these features, larger S_1–T_1 energy gap leads to decrease in the sensitivity of corroles with respect to the heavy atom effects.

This short review aims to summarize the experimental signatures of these specific free base corrole spectral-luminescent and photophysical properties for the first time. The compilation list of the most relevant available photophysical parameters for the forty five free base corrole derivatives with different architecture of the peripheral substitution is presented. The authors have attempted to trace the "structure-property" relationship through the discussion but not to present the exhaustive database of the photophysical properties.

Acknowledgements. This research was funded by the Republic of Belarus State Fundamental Research Program "Convergence-2025", Subprogram "Interdisciplinary Research and New Emerging Technologies", Grant 3.03.10.2.

References

1. Paolesse R., Synthesis of Corroles. In: *The Porphyrin Handbook*, *Vol. 2* (Kadish K.M., Smith K.M., Guillard R., Eds.), San Diego: World Scientific, **2000**, 201–232.
2. Berezin D.B., Karimov D.R., Kustov A.V., *Corroles and Their Derivatives: Synthesis, Properties, Prospects of Practical Applications*, Moscow: LENAND, **2018**, 304 p. [Березин Д.Б., Каримов Д.Р., Кустов А.В. *Корролы и их производные: Синтез, свойства, перспективы практического применения*, URSS. **2018**. 304 с. ISBN 978-5-9710-5293-7].
3. Kruk M.M., Klenitsky D.V., Maes W. *Macroheterocycles* **2019**, *12*, 58–67, doi: 10.6060/mhc190229k.
4. Capar J., Conradie J., Beavers C.M., Ghosh A. *J. Phys. Chem. A*. **2015**, *119*, 3452–3457, doi: 10.1021/jp511188c.
5. Kruk M.M., Ngo T.H., Savva V.A., Starukhin A.S., Dehaen W., Maes W. *J. Phys. Chem. A.* **2012**, *116*, 10704–10711, doi: 10.1021/jp305327c.
6. Beenken W.J.D., Presselt M., Ngo T.H., Dehaen W., Maes W., Kruk M.M. *J. Phys. Chem. A*. **2014**, *118*, 862–871, doi: 10.1021/jp411033h.
7. Fliegl H., Sundholm D. *J. Org. Chem*. **2012**, *77*, 3408–3414, doi:10.1021/jo300182b.
8. Klenitsky D.V., Gladkov L.L., Vershilovskaya I.V., Petrova D.V., Semeikin A.S., Maes W., Kruk M.M. *J. Appl. Spectrosc*. **2022**, *88*, 1111–1118, doi: 10.007/s10812-022-01287-8.
9. Gladkov L.L., Klenitsky D.V., Vershilovskaya I.V., Maes W., Kruk M.M. *J. Appl. Spectrosc.* **2022**, *89*, 426–432, doi: 10.007/s10812-022-01374-w.
10. Baird N.C. *J. Am. Chem.* Soc. **1972**, *94*, 4941–4948, doi:10.1021/ja00769a025.
11. Johnson A.W., Kay I.T. *J. Chem. Soc*. **1965**, *306*, 1620–1629, doi: 10.1039/jr9650001620.
12. Grigg R., Hamilton R. J., Jozefowicz M.L., Rochester C.H., Terrell R.J., Wickwar H. *J. Chem. Soc., Perkin Trans. II* **1973**, *86*, 407–413, doi: 10.1039/P29730000407.
13. Stefanelli M., Pomarico G., Tortora L., Nardis S., Fronczek F.R., McCandless G.T., Smith K.M., Manowong M., Fang Y., Chen P., Kadish K.M., Rosa A., Ricciardi G., Paolesse R. *Inorg. Chem.* **2012**, *51*, 6928–6942, doi: 10.1021/ic3007926.
14. Ziegler C.J., Sabin J.R., Geier III R., Nemykin V.N. *Chem. Commun*. **2012**, *48*, 4743–4745, doi:10.1039/C2CC31146A.
15. Lemon C.M., Halbach R.L., Huynh M., Nocera D.G. *Inorg. Chem*. **2015**, *54*, 2713–2725, doi: 10.1021/ic502860g.
16. Kruk M.M. Ngo T.H., Verstappen P., Starukhin A.S., Hofkens J., Dehaen W., Maes W. *J. Phys. Chem. A* **2012**, *116*, 10695–10703, doi: 10.1021/jp305326x.
17. Ivanova Yu.B., Savva V.A., Mamardashvili N.Zh., Starukhin A.S., Ngo T.H., Dehaen W., Maes W., Kruk M.M. *J. Phys. Chem. A* **2012**, *116*, 10683–10694, doi: 10.1021/jp305325e.
18. Ding T., Aleman E.A., Modarelli D.A., Ziegler C.J. *J. Phys. Chem., A* **2005**, *109*, 7411–7417, doi: 10.1021/jp052047i.
19. Ding T., Harvey J.D., Ziegler C.J. *J. Porphyrins Phthalocyanines* **2005**, *9*, 22–27, doi: 10.1142/ S1088424605000058.
20. Gouterman M. *Optical Spectra and Electronic Structure of Porphyrins and Related Ring*. In: *The Porphyrins* (Dolphin D., Ed.), New York: Acad. Press, **1978**, 3, 1–165, doi: 10.1016/B978-0-12-220103-5.X5001-6.
21. Ajeeb Y.H., Klenitsky D.V., Vershilovskaya I.V., Petrova D.V., Semeikin A.S., Maes W., Gladkov L.L., Kruk M.M. *J. Appl. Spectrosc*. **2020**, *87*, 421–428, doi: 10.1007/s10812-020-01017-y.
22. Ghosh A., Junge K. *Chem. Eur. J.* **1997**, *3*, 823–833, doi: 10.1002/chem.19970030523.
23. Ghosh A., Wondimagegn T., Parusel A.B. *J. Am. Chem. Soc*. **2000**, *122*, 5100–5104, doi: 10.1021/ja9943243.
24. Costa R., Richard G. Geier III, Ziegler C.J. *Dalton Trans.* **2011**, *40*, 4384–4386, doi: 10.1039/C1DT10112A.
25. Mohammad A., Weaver J.S., Gray H.B., Abdelas M., Gross Z. *Tetrahedron Lett.* **2003**, *44*, 2077–2079, doi: 10.1016/S0040-4039(03)00174-6.
26. Ajeeb Y.H., Minchenya A.A., Klimovich P.G., Maes W., Kruk M.M. *J. Appl. Spectrosc.* **2019**, *86*, 788–794, doi: 10.1007/s10812-019-00831-3.
27. Shen J., Ou Z., Shao J., Galezowski M., Gryko D.T., Kadish K.M. *J. Porphyrins Phthalocyanines* **2007**, *11*, 269–276, doi: 10.1142/S1088424607000321.
28. Shakel A.Yu., Sokhibova A.M., Petrova D.V., Kruk M.M. *J. Appl. Spectrosc*. **2024**, *91*, 177–183.
29. Kruk M.M. *J. Appl. Spectrosc*. **2022**, *89*, 624–630, doi: 10.1007/s10812-022-01402-9.
30. Nappa M., Valentine J.S. *J. Am. Chem. Soc*. **1978**, *100*, 5075–5080, doi: 10.1021/ja00484a027.
31. Lakowicz J.R. *Principles of Fluorescence Spectroscopy*. New York: Plenum Press, **1983**, 496 p.
32. Takeda J., Sato M. *Chem. Lett*. **1995**, *11*, 971–972, doi: 10.1246/cl.1995.971.
33. Knyukshto V.N., Gladkov L.L., Maes W., Kruk M.M. *J. Appl. Spectrosc.* **2023**, *90*, 507–514, doi: 10.1007/s10812-023-01560-4.
34. Röder B., Büchner M., Rückmann I., Senge M.O. *Photochem. Photobiol. Sci.* **2010**, *9*, 1152–1158, doi: 10.1039/C0PP00107D.
35. Senge M.O., *Highly Substituted Porphyrins*. In: *The Porphyrin Handbook*, Vol. 1 (Kadish K.M., Smith K.M., Guillard R., Eds.), San Diego: World Scientific, **2000**, 239–347.
36. Shelnutt J.A., Song X., Ma J., Jia S., Jentzen W., Medforth C.J. *Chem. Soc. Rev*. **1998**, *27*, 31–41, doi: 10.1039/A827031Z.
37. Simkhovich L., Goldberg I., Gross Z. *J. Inorg. Biochem.* **2000**, *80*, 235–238, doi: 10.1016/S0162-0134(00)00077-5.
38. Ajeeb Y.H., Karlovich T.B., Gladkov L.L., Maes W., Kruk M.M. *J. Appl. Spectrosc*. **2019**, *86*, 389–395, doi: 10.1007/s10812-019-00831-3.
39. Knuykshto V.N., Ngo T.H., Dehaen W., Maes W., Kruk M.M. *RSC Adv.* **2016**, *6*, 43911–43915, doi: 10.1039/c6ra06196f.
40. Sinha W., Ravotto L., Ceroni P., Kar S. *Dalton Trans*. **2015**, *44*, 17767–17773, doi: 10.1039/C5DT03041B.
41. Tanabe M., Matsuoka H., Ohba Y., Yamauchi S., Sugisaki K., Toyota K., Sato K., Takui T., Goldberg I., Saltsman I., Gross Z. *J. Phys. Chem. A.* **2012**, *116*, 9662–9673. doi: 10.1021/jp3071037
42. Vestfrid J., Botoshansky M., Palmer J.H., Durrell A.C., H.B. Gray H.B., Gross Z. *J. Am. Chem. Soc.* **2011**, *133*, 12899–12901, doi: 10.1021/ja202692b.
43. Rabinovich E., Goldberg I., Gross Z. *Chem. Eur. J.* **2011**, *17*, 12294–12301, doi: 10.1002/chem.201102348.
44. Senge M.O., MacGovan S.A., O'Brien J. *Chem. Commun.* **2015**, *51*, 17031–17063, doi: 10.1039/c5cc06254c.
45. Mc Glynn S.P., Azumi T., Kinoshita M. *Molecular Spectroscopy of the Triplet States*, New Jersey: Prentice-Hall, Inc., **1969**, 448 p.

46. Vershilovskaya I.V., Stefani S., Verstappen P., Ngo T.H., Scheblykin I.G., Dehaen W., Maes W., Kruk M.M. *Macroheterocycles* **2017**, *10*, 257–267, doi: 10.6060/ mhc160962n.
47. Maes W., Ngo T.H., Vanderhaeghen J., Dehaen W. *Org. Lett.* **2007**, *9*, 3165−3168, doi: 10.1021/ol071226a.
48. Ventura B., Esposti A.D., Kozharna B., Gryko D.T., Flamigni L. *New. J. Chem.* **2005**, *29*, 1559–1566, doi: 10.1039/B507979A.
49. Nastasi F., Campagna S., Ngo T., Dehaen W., Maes W., Kruk M. *Photochem. Photobiol. Sci.* **2011**, *10*, 143– 150, doi: 10.1039/c0pp00282h.
50. Kruk M.M. *Proc. BSTU*, *Ser. 3, Physics and Mathematics. Informatics* **2023**, Is. (1), 29 – 33, doi: 10.52065/2520-6141-2023-266-1-6.
51. Paolesse R., Marini A, Nardis S., Froiio A., Mandoj F., Nurco D.J., Prodi L., Montalti M., Smith K. M. *J. Porphyrins Phthalocyanines* **2003**, *7*, 25–36, doi: 10.1142/S1088424603000057.
52. Kruk M.M., Klenitsky D.V., Gladkov L.L., Maes W. *J. Porphyrins Phthalocyanines* **2020**, *24*, 765–774, doi: 10.1142/S1088424619501797.
53. Ngo T.H., Puntoriero F., Nastasi F., Robeyns K., Van Meervelt L., Campagna S., Dehaen W., Maes W. *Chem. Eur. J.* **2010**, *16*, 5691–5705, doi: 10.1002/chem.201000008.
54. Paolesse R., Sagone F., Macagnano A., Boschi T., Prodi L., Montalti M., Zacceroni N., Boletta F., Smith K.M. *J. Porphyrins Phthalocyanines* **1999**, *3*, 364–370, doi: 10.1002/ (SICI)1099-1409(199906).
55. Canard G., Gao Di, D'Aleo A., Giorgi M., Dang F.-X., Balaban T.S. *Chem. Eur. J.* **2015**, *21*, 7760-7771, doi: 10.1002/ chem.201406369.
56. Murov S.L., Carmichael I., Hug G.L. *Handbook of Photochemistry, 2-nd ed.,* New York: Marcel Dekker **1993**, 420 p.
57. Solovyov K.N., Borisevich E.A. *Usp. Fiz. Nauk*. **2005**, *175*, 247–270, doi: 10.1070/pu2005 v048n03abeh001761.
58. Azenha E.G., Serra A.C., Pineiro M., Pineira M.M., Seixas de Melo J., Arnaut L.G., Fromosinho S.J., Rocha Gonsalves A.M.d'A. *Chem. Phys*. **2002**, *280*, 177–190, doi: 10.1016/S0301-0104(02)00485-8.
59. Shakel A.Yu., Sokhibova A.M., Petrova D.V., Semeikin A.S., Kruk M.M. *Proc. BSTU*, *Ser. 3, Physics and Mathematics. Informatics* **2022**, Is. (2), 36–42, doi: 10.52065/2520-6141-2022-260-2-36-42.
60. Soll M., Sudhakar K., Fridman N., Müller A., Röder B., Gross Z. *Org. Lett.* **2016**, *18*, 5840–5843, doi: 10.1021/ acs.orglett.6b02877.
61. Ooi S., Yoneda T., Tanaka T., Osuka A. *Chem. Eur. J*. **2015**, *21*, 7772–7779, doi: 10.1002/chem.201500894.
62. Ueta K., Tanaka T., Osuka A. *Chem. Lett.* **2018**, *47*, 916–919, doi: 10.1246/cl.180309.
63. Ooi Sh., Tanaka T., Osuka A. *Eur. J. Org. Chem.* **2015**, 130–134, doi: 10.1002/ejoc.201403217.
64. Ueta K., Tanaka T., Osuka A. *Molecules* **2019**, 642, doi: 10.3390/molecules24030642.
65. Ngo T.H., Nastasi F., Puntoriero F., Campagna S., Dehaen W, Maes W. *J. Org. Chem*. **2010**, *75*, 2127–2130, doi: 10.1021/jo902709c.
66. Vestfrid J., Goldberg I., Gross Z. *Inorg. Chem.* **2014**, *53*, 10536–10542, doi: 10.1021/ic501585a.
67. Karimov D.R., Barannikov V.P., Mal'tseva O.V., Kumeev R.S., Berezin D.B. *Izv. Vyssh. Uchebn. Zaved., Khim. Khim. Tekhnol. [ChemChemTech]* **2011**, *54*(4), 26–33.
68. Sagun E.I. *Khim. Fiz.* **1990**, *9*, 764–771.
69. Bonnett R. *Chemical Aspects of Photodynamic Therapy,* Amsterdam: Gordon and Breach Science Publishers, **2000**, 305 p.
70. Teo R.D., Hwang J.Y., Termini J., Gross Z., Gray H.B. *Chem. Rev.* **2017**, *117*, 2711–2729, doi: 10.1021/acs.chemrev.6b00400.
71. Kruk M.M. *Structure and Optical Properties of Tetrapyrrolic Compounds*. Minsk: BSTU Publ., **2019**, 216 p. [Крук Н.Н. *Строение и оптические свойства тетрапиррольных соединений.* Минск: БГТУ, **2019**. 216 с.], *https://elib.belstu.by/handle/123456789/36702.*

Received 10.04.2024
Accepted 01.05.2024